Postnatal *Tshz3* Deletion Drives Altered Corticostriatal Function and Autism Spectrum Disorder-like Behavior

SUPPLEMENT 1

SUPPLEMENTAL METHODS AND MATERIALS

Generating Tshz3-*deficient mice*

A 129/SvEvTac mouse BAC clone (RPCI22 library, resource CHORI BACPAC) containing *Tshz3* was identified by Southern hybridization with a *Tshz3* cDNA. A DNA fragment of the *Tshz3* gene (18.5 kb) containing exon 2 was isolated by gap repair (1) using a vector including a DTA cassette for negative selection in embryonic stem (ES) cells (2). First, two mini targeting vectors were constructed, which consisted of a dual promoter kanamycin/neomycin selection cassette, frt and loxP sequences with flanking sequences from the *Tshz3* gene. The first mini targeting vector was inserted into a low homology region downstream of the coding exon 2 and 3′-UTR sequences of *Tshz3*. Homologous recombination in bacteria enables the sequence-specific integration of desired DNA fragments independent of restriction enzymes. Regions of 30-50 bp homology at the 5′ and 3′ ends of a fragment are sufficient to achieve a high recombination frequency. In order to recombine a DNA fragment, the vectors were transformed into DY380 *E. coli* bacteria that carry the red genes necessary for recombination (exo and pol) under the control of a temperature-sensitive λ repressor, due to the fact that permanent expression of the red genes is lethal for bacteria (3). The floxed neomycin cassette was removed using bacterially expressed Cre recombinase, leaving behind a loxP site downstream of exon 2 and an additional BamHI site immediately 5′, which was used later for Southern blot analysis of ES cell clones. In the 5′ region of *Tshz3*, the second mini targeting vector was introduced,

resulting in a targeting vector containing a loxP-frt-neomycin-frt cassette 5′ of exon 2 and a single loxP site 3′ of exon 2. This was introduced by electroporation into R1 ES cells, and homologous recombinants screened by Southern blotting. Following removal of the frt-flanked neomycin cassette through germline deletion in mice, animals with the resulting *Tshz3*^{flox} allele were established for conditional deletion. Conditional mouse mutants with **p**ost**n**atal loss of *Tshz3* in the **c**orte**x** (***Tshz3-pnCxKO***) were obtained by crossing *Tshz3*$^{flox/flox}$ mice with *CaMKIIalpha-Cre* mice (4) that express the CRE-recombinase in glutamatergic CPNs (see **Supplemental Figure S5**), as well as in the hippocampus and amygdala, from P2-P3 onward. Notably, striatal SPNs do not express TSHZ3 (5, 6), thus this model should not affect these cells.

Mouse genotyping

Animals carrying the *Tshz3*^{flox} allele were genotyped using the following protocol: forward primer: 5′ - GTGACACACTCTGTGCCCTGTTTTG - 3′; reverse primer: 5′ - CCAACCTGGTTGTCTCTGCTTGCTT - 3′. Fragment sizes were: 760 bp (floxed), 629 bp (wild-type). A 400 bp non-specific band was also noted on occasion. For animals carrying the *Tshz3*$^{\Delta}$ allele, genotyping was as follows: Forward primer: 5′ - TGAGTCTGTAAGGCTAGCACCTGTG - 3′; Reverse primer: 5′ - CCAACCTGGTTGTCTCTGCTTGCTT - 3′. Fragment size of recombined allele: 457 bp. For both protocols, following melting at 94°C, primers were annealed at 59°C and elongated at 72°C for 60 sec +1 sec/cycle, total of 35 cycles. Mg^{2+} was at 4 mM. *Tshz3-pnCxKO* mice were obtained by crossing female *Tshz3*$^{flox/flox}$ with male *CaMKIIalpha-Cre* mice, the latter expressing Cre-recombinase in projection neurons from P2-P3 onward, leading to the conditional early postnatal deletion of *Tshz3* in CaMKIIalpha-expressing neurons, including CPNs (4). Control mice were *Tshz3*$^{flox/flox}$;Cre-negative mice.

RNA sequencing analysis

Three independent replicates, each containing cortices from 3-4 mice (P34), were prepared for analysis. For each sample, RNA sequencing libraries were constructed from 1 µg of total RNA with the Truseq stranded mRNA sample preparation kit (low throughput protocol) from Illumina. After poly-A based mRNA enrichment (poly-T oligo attached magnetic beads) and mRNA fragmentation (using divalent cations under elevated temperature), RNA fragments were copied into first strand cDNA using reverse transcriptase and random primers; the second strand cDNA was synthesized subsequently. These cDNA fragments were added with a single 'A' base and then ligated with the adapter. The products were purified and enriched with 15 PCR cycles. The final cDNA libraries were validated with a DNA 1000 Labchip on a Bioanalyzer (Agilent) and quantified with a KAPA qPCR kit. For one sequencing lane, six libraries were pooled in equal proportions, denatured with NaOH and diluted to 7 pM before clustering. Clustering and 50 nt single read sequencing were performed according to the manufacturer's instructions. Image analysis and basecalling were performed using the HiSeq Control software and Real-Time Analysis component. Data quality was assessed using fastqc from the Babraham Institute and the Illumina software SAV (Sequence Analysis Viewer). Demultiplexing was performed using Illumina's sequencing analysis software (CASAVA 1.8.2). A splice junction mapper, TopHat 2.0.9 (7) (using Bowtie 2.1.0 (8)), was used to align RNA-Seq reads to mouse genome (mm10) with a set of gene model annotations (genes.gtf downloaded from UCSC on March 6 2013). Final read alignments having more than 3 mismatches were discarded. Then, the counting was performed with HTSeq count 0.5.3p9 (union mode). Before statistical analysis, genes with less than 15 reads (adding all the analyzed samples) were filtered and thus removed.

Immunohistochemistry and histology

P28-old mice were anesthetized (ketamine + xylazine, 100 + 10 mg/kg, respectively, i.p.) prior to transcardial perfusion with phosphate-buffered saline (PBS) followed by 4% paraformaldehyde (PFA) in 0.1 M phosphate buffer (PB). Brains were removed and post-fixed in 4% PFA for at least 2 h before being sectioned in a coronal plane. Sections were incubated overnight at 4°C with primary antibodies (see below). The following primary antibodies were used: NeuN (mouse, 1/500, Mab377 Millipore), BCL11B (1:1000, rat, Abcam), VGLUT1 (rabbit, 1:1000, Synaptic Systems), TSHZ3 (guinea-pig, 1:2000 (9)). Immunostaining with anti-TSHZ3 was obtained from cryostat sections of brains immediately harvested after euthanasia and frozen in dry ice. Sections were fixed with 4% paraformaldehyde for 15 min, and washed twice for 5 min in PBS before incubation procedures. Secondary antibodies were: donkey anti-rabbit Cy3, goat anti-mouse Alexa Fluor 488, goat anti-rat Alexa Fluor 555 (Molecular Probes), donkey anti-guinea pig Cy3 (Jackson ImmunoResearch Laboratories), all diluted 1:1000 and incubated overnight at 4°C. Images were acquired using a laser scanning confocal microscope (Zeiss LSM780 with Quasar detection module) and processed using Adobe Photoshop. Spectral detection bandwidths (nm) were set at 411-473 for DAPI, 498-568 for GFP and 568-638 for Cy3; pinhole was set to 1 Airy unit. Unbiased stereological counting of NeuN, BCL11B and VGLUT1-positive neurons was done from confocal images with ImageJ software (see figure legends for frame details).

Retrograde tracing

P28-old mice under anesthesia (see above) received stereotaxic injections of 0.3 µl of cholera toxin subunit B (CT-B) conjugated with Alexa Fluor 555 at 1% in 0.12 M PB, pH 6 (List Biological Laboratories) in the striatum (A: +1 mm L: +1.6 mm DV: -2 mm from dura) using

the bregma coordinates (10). At 10 days post-injection, animals were anesthetized and perfused transcardially with 4% PFA (see above).

Electrophysiology

Slices were obtained from P21-28 mouse brains by a vibratome (Leica S1000) in ice-cold solution containing (in mM): 110 choline, 2.5 KCl, 1.25 NaH_2PO_4, 7 $MgCl_2$, 0.5 $CaCl_2$, 25 $NaHCO_3$, 7 glucose, pH 7.4. Slices were then kept at room temperature in oxygenated artificial cerebrospinal fluid (ACSF), whose composition was (in mM): 126 NaCl, 2.5 KCl, 1.2 $MgCl_2$, 1.2 NaH_2PO_4, 2.4 $CaCl_2$, 11 glucose, and 25 $NaHCO_3$, pH 7.4. I-V relationship for CPNs and SPNs was obtained in current-clamp mode by injecting hyperpolarizing and depolarizing current steps ($\Delta I = \pm 50$ pA, 800 ms). Input resistance (Ri) was calculated by linear regression analysis, i.e. as the slope of the linear best fit of the I-V relationship. To classify L5 CPNs as PT or IT, we measured and summed the values of the "sag & rebound" triggered by a hyperpolarizing current step (-250 pA, 800 ms), and the after-hyperpolarization (AHP) triggered by a depolarizing current step (+250 pA, 800 ms). The average value of the "sag & rebound + AHP" sum was 4.2 mV in both control and mutant. This value was taken as a cut-off, because it let us discriminating between PT (sum > 4.2 mV), which distinctly show the sag & rebound and the AHP, from IT CPNs (< 4.2 mV), in which the value of at least one these parameters is negligible. For calculating paired-pulse ratio (PPR), EPSC and IPSC amplitude was measured on 6 averaged traces at each different inter-pulse interval. For analyzing mEPSCs, the detection threshold (around 3-4 pA) was set to twice the noise after trace filtering (Boxcar low-pass), and only cells exhibiting stable activity and baseline were taken into account. To calculate NMDA/AMPA ratio (11), the AMPA component of the EPSC was measured at the peak at a holding potential of -60 mV, while the NMDA component was measured at +40 mV and 40 ms after the stimulation artifact, when the AMPA component is

negligible (**Figure 4D**). EPSC amplitude for monitoring long-term depression and potentiation (LTD and LTP, respectively) was measured on averaged traces (6 per minute) to obtain time-course plots and to compare this parameter before (baseline) and after induction protocols. The induction protocol for corticostriatal LTD of in 3 trains at 100 Hz, 3 s duration, 20 s interval, at half intensity compared to baseline. LTP induction protocol was identical but, during each train, SPNs were depolarized to -10 mV to allow strong activation of NMDA receptors (12). Electrophysiological data were analyzed offline by Clampfit 10.2 (Molecular Devices, USA) and MiniAnalysis 6.0 (Synaptosoft, USA) software.

ASD-relevant behavior testing

We used male mice aged 101-127 days in order to maximize the reliability for behavioral assessments (13, 14). Grouped mouse males frequently display agonistic behavior (15, 16). Accordingly, several of the males used here displayed aggressive behavior and they could not be housed together. Moreover, as social isolation generates undesirable physiological and brain effects that can be permanent (17), we could not isolate these males. Thus, in order to avoid these possible biases, we choose the solution to house each male to be tested with a female. Transparent 35 x 20 x 18 cm cages were used with poplar woodchip bedding, a dome house for enrichment, food (Harlan Global Diet 2018) and water ad lib, and a 12/12-hour light/dark period with lights on at 7 a.m.

Marble burying test. This test is an indirect measure of burrowing behavior (pushing and digging) that quantifies repetitive and persevering behavior (18). The number of covered marbles depends on the frequency of pushing and digging episodes. The cages (40 x 40 x 18 cm) are filled with usual litter (5 cm thick). After a 10 min habituation period in a new cage (brightness on the ground 70 lux), the tested mouse is restricted to a corner of the cage with a mobile partition, while twenty marbles (1 cm in diameter) in 4 evenly spaced rows of 5 marbles

are placed on top of the bedding. The partition is removed and the mouse is left alone for 30 min. A marble is scored 3 when completely covered, 2 when buried two-thirds deep and 1 when half-buried. The individual score is the sum of the scores of the 20 marbles.

Hole-board test. Stereotyped behavior was explored in an automated hole-board. The apparatus consists of a grey vinyl plastic board (40 x 40 cm) with 16 equidistant holes (3.5 cm diameter) forming 4 rows and 4 columns. Photobeams crossing the holes allow automatic counts of nose pokes for each hole. The board was located in the center of a room (70 lux). The mouse was always placed in the same corner of the board and allowed to explore for 10 min. We measured the total number of nose dips distinguishing the exploratory dips from the stereotyped dips for each mouse (19). A stereotypy was counted when the mouse poked the nose twice consecutively in the same hole within 2 s. Each session was filmed and the stereotypies were counted during two displays. The number of non-stereotyped dips was automatically recorded.

Open field exploration test. Mice were placed at the periphery of a white cylinder (100 cm diameter), divided in three virtual concentric zones of equal surface (150 lux on the ground). The total distance walked, the number of zone crossings and the time spent in the center of the arena were video-recorded for 20 min and used to measure ambulatory activity, field of interest and anxiety-like behavior, respectively. The leanings and rearing were counted during the test. The other measures were counted automatically via the Viewpoint-Behavior technologies system (http://www.viewpoint.fr/news.php).

Sociability and social novelty preference test. The sociability (number of interactions towards a conspecific) and the interest in social novelty (increased number of interactions towards an unknown conspecific) were measured according to the principles of the three-chamber test (20, 21) but in a different two-chamber set up (5, 22) with opaque walls. The behavior was video-recorded via a camera located 170 cm above the set up (Viewpoint-Behavior technologies). After a 5 min habituation in the smaller compartment, the assay consisted of three successive

sessions of 10 min, during which the tested mouse was allowed to explore the total device and the numbers of nose pokes on the two pencil boxes were counted. In the first session (habituation), the two boxes were empty. In the second session (sociability), one box contained a stranger C57BL/6J (B6) male and the other a lure. In the third session (social novelty), the C57BL/6J (B6) was left in its box and the lure was replaced by a stranger SWR male. Before the second and the third sessions, the tested mouse was gently pushed into the smaller compartment while positioning the B6 and the SWR conspecifics (60 lux on the ground).

Elevated plus maze. The elevated plus maze provides a measure of anxiety-like behavior based on the avoidance of a condition generating anxiety. We used a plus-shaped device with two open and two closed arms, elevated 80 cm from the floor. Each mouse was placed in the central area of the maze (6×6 cm), with its head towards the enclosed arm, and allowed to move freely for 15 min. The walked distance (cm) in the opened and closed arms was measured by a video tracking system.

Morris water maze

This test measures the ability of the mouse to find a submerged resting platform concealed beneath opaque water, an exercise requiring the use of extra-maze visual cues which are provided in the room (23, 24). The platform is a glass cylinder (7 cm diameter) positioned 23 cm from the edge of a 100 cm diameter circular tank filled with water at 26 ± 1°C and light at 70 lux on the surface (25). Each mouse performed 7 blocks of 4 trials each: one block on day 1, and two blocks every day for 3 successive days (one in the morning and one in the afternoon). A trial lasted 90 s when the mouse failed to reach the platform. We considered that the mouse had reached the platform when it stayed on the platform for 5 s at least. We presented a small metal shelf to the mouse 5 cm above the platform at the end of each trial of the first block (shaping). The mouse climbed on it and was transferred in a cage with dry sawdust for 120 s.

At the end of a trial of the other blocks we presented the shelf 30 cm from the mouse but not above the platform. The location of the platform was no longer signaled. We had previously assigned 4 virtual cardinal points to the tank, each being the starting point for a trial. The starting point for each trial was chosen randomly and within a block the mouse never started more than once from the same virtual cardinal point. We measured and reported the "time to reach the hidden platform" over the 7 blocks. Strains can achieve different performance levels between blocks, but without a cumulative reduction in the time to reach the platform, which is the criterion to identify learning process. We computed "the slopes of the learning curves", a negative slope indicating learning behavior (26). The probe-test procedure, conducted after removing the platform, was done 24 h after block 7 to meet the requirements for reference memory (27) and lasted 90 s. The mouse was placed in the center of the tank, and we measured the time of first crossing the virtual annulus corresponding to the location of the platform. We subjected a group of naïve *Tshz3-pnCxKO* mice and a group of wild-type mice to the visible-platform version of the test, with the platform 5 mm above non-opacified water to check whether the differences in the time to reach the platform were due to vision and/or swimming abilities rather than learning ability. The time to reach the platforms was automatically measured using a video tracking setup (Viewpoint-Behavior technologies).

Motor skills testing

Hind limb coordination was measured in the notched bar test used to assess gait impairment (number of hind paw slips) (28). A solid bar with a smooth surface was used for shaping. Two experimenters stood either side of the carved bar to count the number of times the mouse slipped over five trials.

Sensory functions testing

We have examined vision, audition and olfaction in the mice of the two groups, since the results obtained in different tasks depend on the integrity of these functions. The mice were subjected for sensorial controls within two weeks after the last experimental testing.

Visual performance. We took the mouse by the tail between the thumb and the forefinger and lifted it. The tip of a pencil was approached to its eyes, without touching the vibrissae. The mouse raised the head, extended the forelimbs and grasped or tried to grasp the pen when the visual function was undamaged. The scores were: raising the head (1), extending the forelimbs (2) and grasping or trying to grasp the pen (3). The task was administered four times at 10 min intervals. The score was the sum of the three last trials. Another estimate of visual impairment was provided by the use of the metal shelf when presented distally.

Auditory performance. The Preyer response was used for detecting potential auditory impairment. It consisted of pinna twitching and going flat backwards against the head as a reaction to sound. The response was validated as an indicator of the auditory acuity by measuring the associated averaged evoked auditory potential. We evaluated the responses to stimulations in the ultrasound bandwidth. The mice, placed in soundproof chamber, received sounds from two commercial dog whistles (10 cm from the ear). The first produced 50 ± 0.08 kHz and the second 35 ± 0.10 kHz sounds. The mouse received 5 stimulations from each whistle at 3 min intervals. The Preyer response was scored 1 for a partial response (ear startling) and 2 for a full response (pinna going flat backwards against the head).

Olfactory capacities screening. The olfactory habituation/dishabituation test was performed according to the previously described classical protocol (29). Non-social odors included water, and synthetic violet and vanilla aromas that were sugar-free. The mouse was alone in a ventilated room during the test.

SUPPLEMENTAL FIGURES

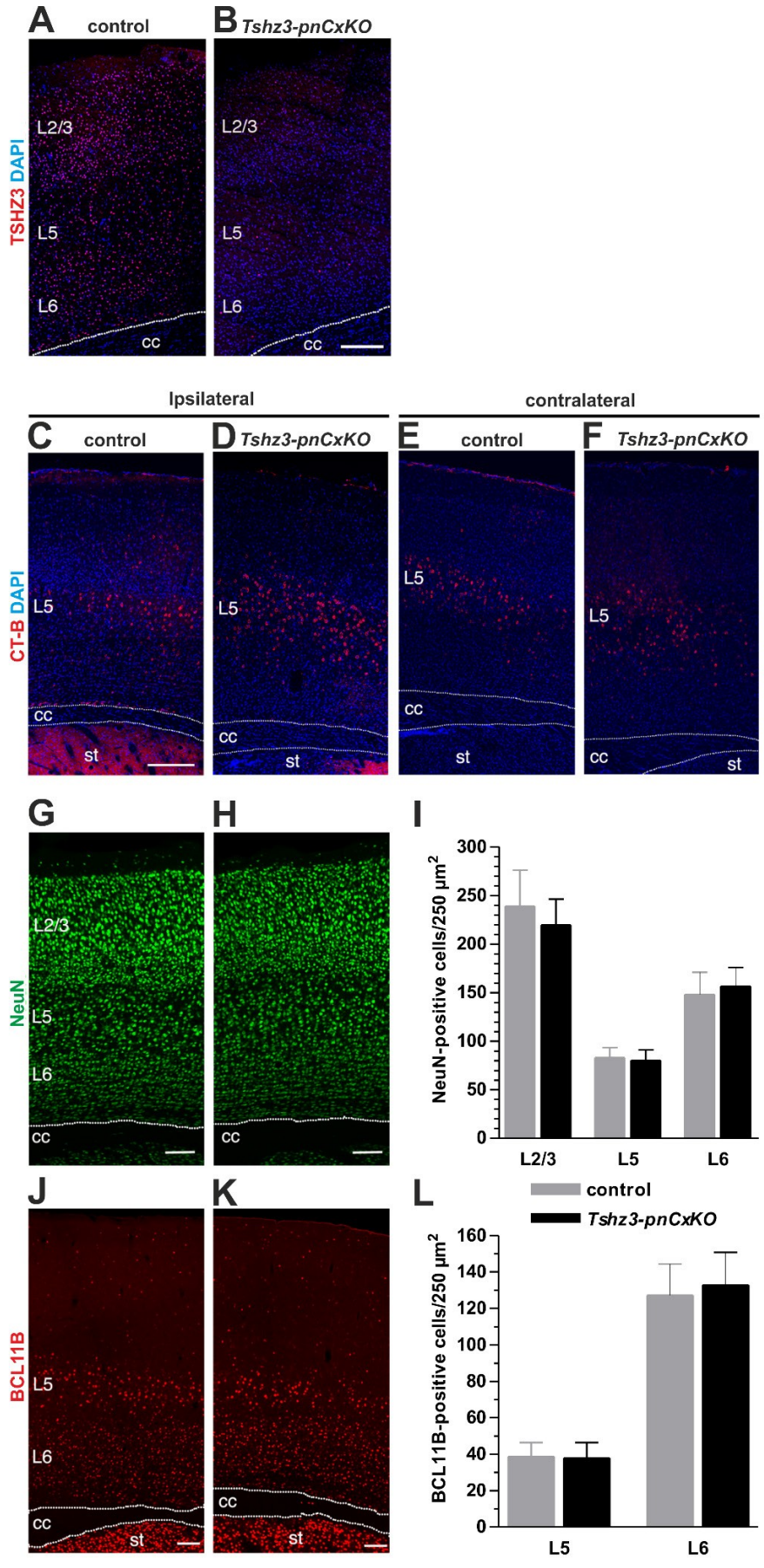
A control
B Tshz3-pnCxKO
TSHZ3 DAPI
L2/3
L5
L6
cc
Ipsilateral
contralateral
C control
D Tshz3-pnCxKO
E control
F Tshz3-pnCxKO
CT-B DAPI
st
G
H
I
NeuN
NeuN-positive cells/250 µm2
300
250
200
150
100
50
0
L2/3
L5
L6
J
K
L
BCL11B
control
Tshz3-pnCxKO
BCL11B-positive cells/250 µm2
160
140
120
100
80
60
40
20
0

Supplemental Figure S1. TSHZ3 expression and consequences of conditional *Tshz3* deletion in the primary motor and somatosensory regions of the cortex at P28. DAPI staining is shown in blue in a-f. (**A**, **B**) TSHZ3-positive cells (red) were counted in random squares of 300 μm^2 in the neocortex. Their number is dramatically decreased (-96.85 ± 1.42%) in *Tshz3-pnCxKO* mice (**B**) *vs*. control (**A**). The presence of the corticostriatal projection is shown by retrograde labeling of ipsilateral (**C**, **D**) and contralateral (**E**, **F**) L5 cortical neurons after unilateral injection of cholera toxin B (CT-B) into the striatum in both control (**C**, **E**) and *Tshz3-pnCxKO* (**D**, F) mice. (**G, H, J, K**) Representative images of immunofluorescence for NeuN (**G, H**) and BCL11B (**J, K**) on coronal sections of control and *Tshz3-pnCxKO* adult brains (P28). (**I**, **L**) Graphs indicate for each layer the number of NeuN and BCL11B-positive cells (means ± s.e.m.) that were counted in random squares of 250 μm^2 in L6, L5, and L2/3, respectively. No significant differences in cell number were found in *Tshz3-pnCxKO vs*. control. (**I**) NeuN–positive counting was done from a minimum of 29 sections from 4 mice per genotype (L6: 148.1 ± 22.8 *vs*. 156.3 ± 19.5, $P = 0.123$; L5: 83.0 ± 10.5 *vs*. 80.2 ± 11.0, $P = 0.279$; L2/3: 238.8 ± 37.0 *vs*. 219.4 ± 26.8, $P = 0.09$). (**I**) BCL11B-positive cell counting was done from 32 sections from 3 mice per genotype (L6: 127.2 ± 17.2 *vs*. 132.8 ± 17.9, $P = 0.187$; L5: 38.7 ± 7.6 *vs*. 37.9 ± 8.4, $P = 0.665$). Scale bars: 200 µm. Abbreviations: cc: corpus callosum; L2/3, L5 and L6: cortical layers 2/3, 5 and 6; st: striatum.

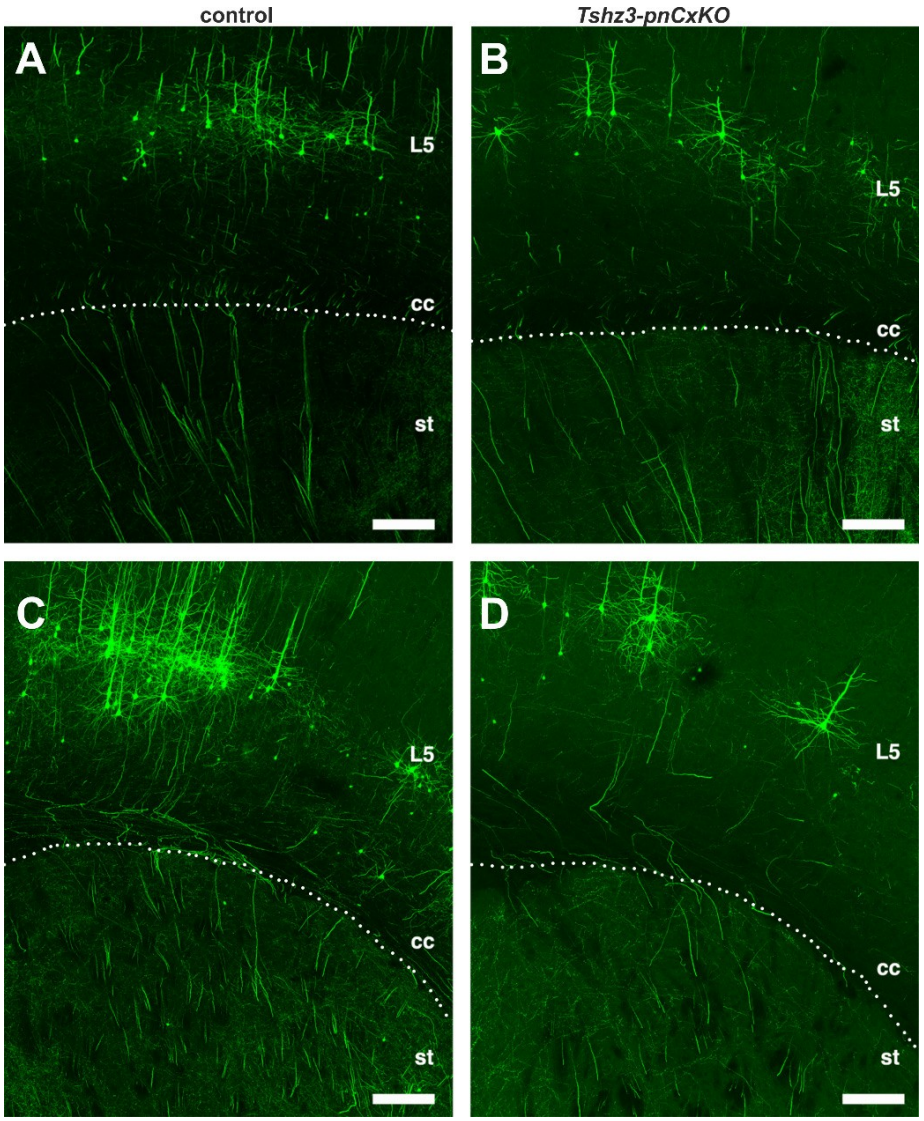

Supplemental Figure S2. Normal L5 corticostriatal projections of *Tshz3-pnCxKO* mice at the level of the primary motor and somatosensory cortex. (**A-D**) *Thy1-GFP* staining on parasagittal (**A**, **B**) and coronal (**C**, **D**) sections in control (**A**, **C**) and *Tshz3-pnCxKO* (**B**, **D**) mice does not show gross modifications of L5 neurons and their axons projecting to the striatum (delimited by the dotted line). Scale bars: 200 µm (**A-D**). Abbreviations: cc: corpus callosum; L5: cortical layer 5; st: striatum.

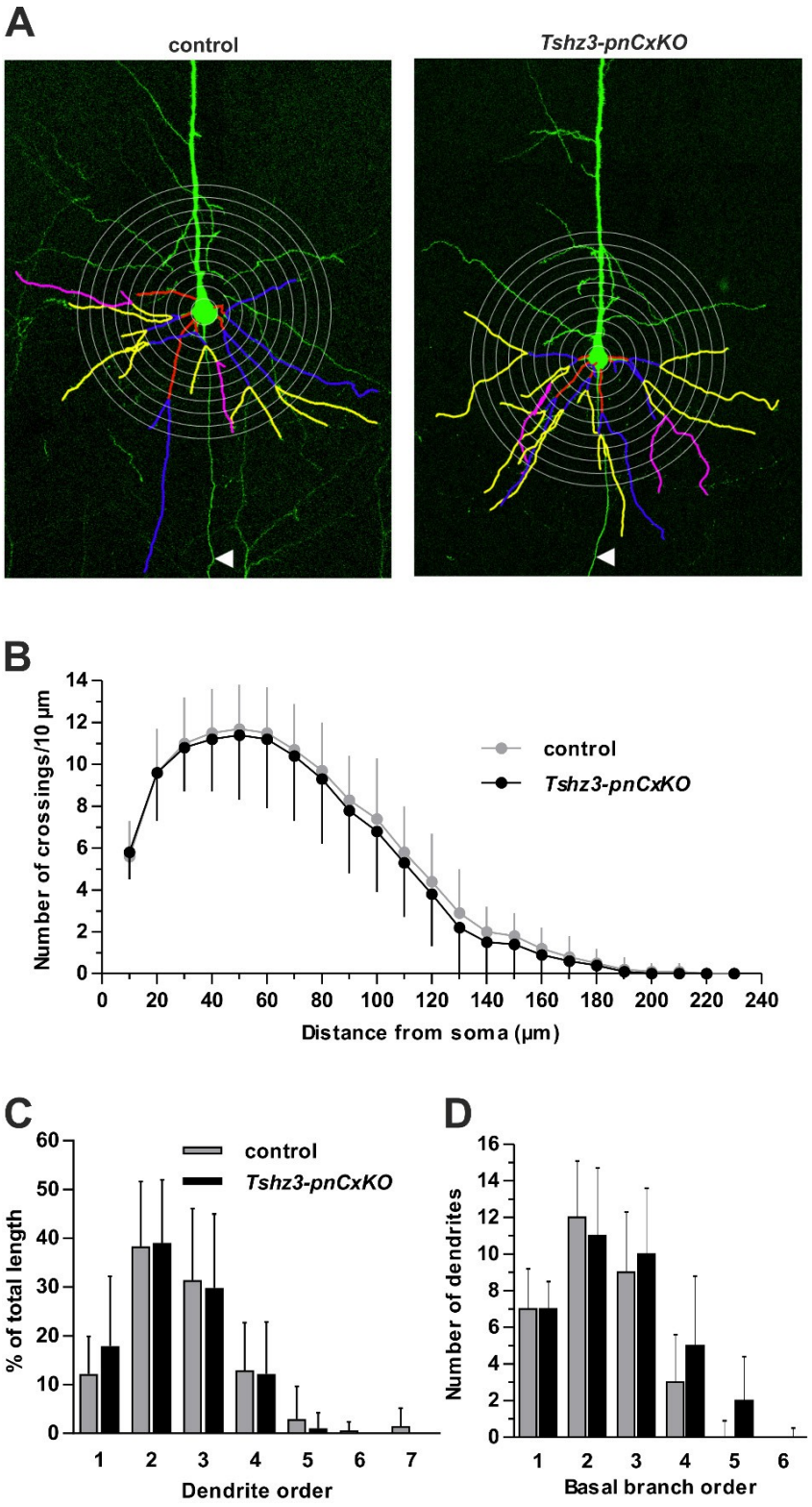

Supplemental Figure S3. Preserved morphology and dendritic complexity of CPNs in *Tshz3-pnCxKO* mutant compared to control mice. (**A**) Basal compartment Scholl analysis of representative control and *Tshz3-pnCxKO* mutant THY1-GFP-M-positive L5 pyramidal

neurons of the primary motor and somatosensory cortex. (**B**) Basal compartment Scholl analysis showing the number of dendrite crossing as a function of distance from the soma. Mutant GFP-positive neurons have no significant difference compared to control. (**C**) Percent dendritic length as a function of branch order in the basal compartment. The dendritic complexity is not significantly affected in mutant GFP-positive neurons. (**D**) The number of dendrites as a function of branch order in basal compartment is similar in control and mutant GFP-positive neurons. (**B-D**) data are expressed as means ± s.e.m.

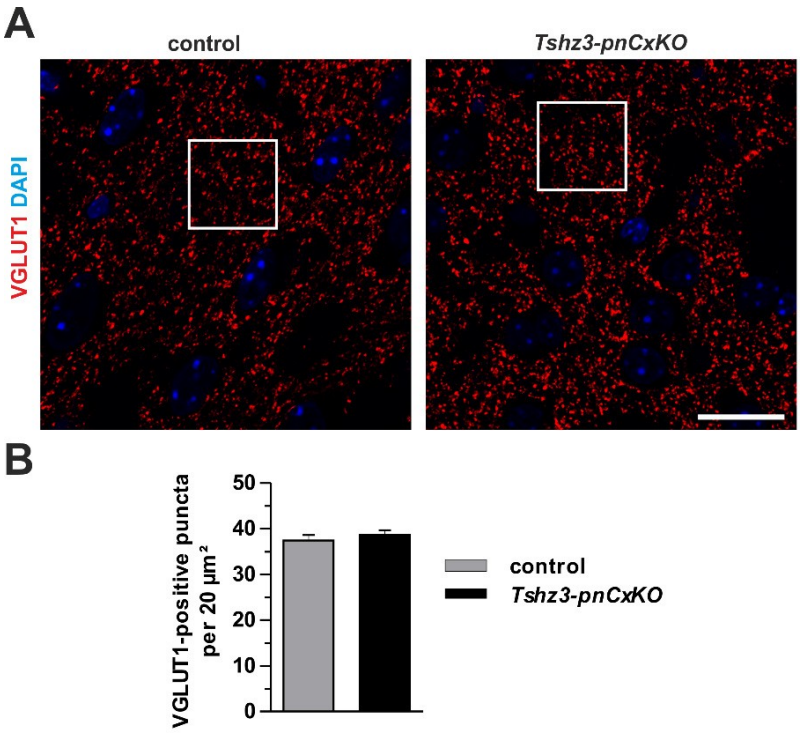

Supplemental Figure S4. Striatal VGLUT1 staining. (**A**) VGLUT1 immunostaining (red) and DAPI staining (blue) on sections of control and *Tshz3-pnCxKO* adult striatum (P28). Scale bar = 5 µm. (**B**) Quantification of the number of VGLUT1-positive puncta in 20 µm^2 squares as shown in above images in control (n = 59) and *Tshz3-pnCxKO* (n = 56); 37.41 ± 1.16 *vs.* 38.65 ± 1.01 puncta/20 µm^2, respectively (means ± s.e.m.; 9 sections from 3 mice for each group).

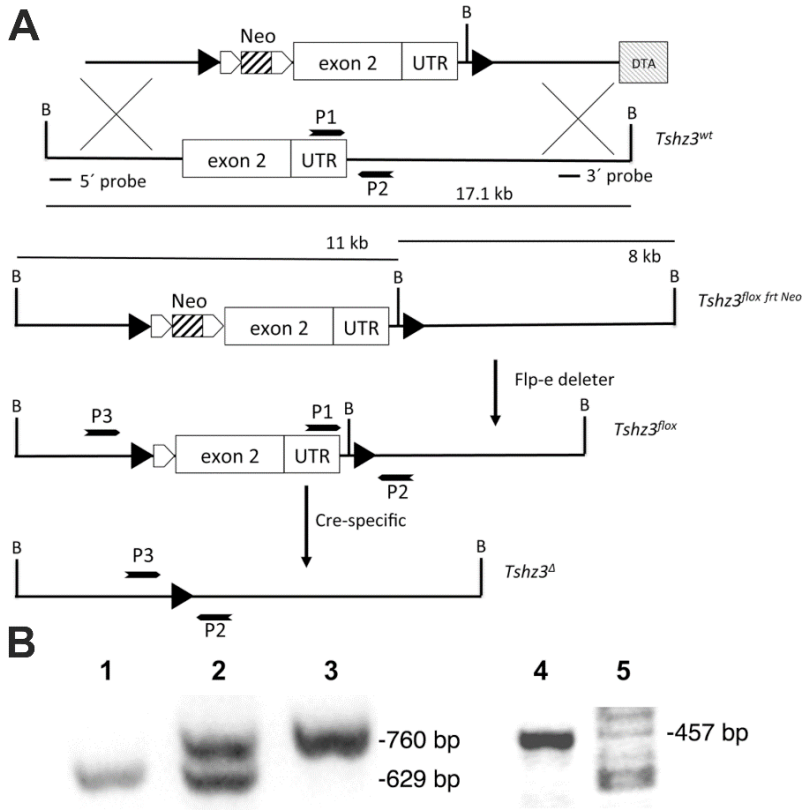

Supplemental Figure S5. Generating *Tshz3*-deficient mice: gene targeting of *Tshz3* by conditional mutagenesis. (**A**) The targeting vector used to generate the conditional *Tshz3*^{flox} allele is shown at the top. *loxP* and *frt* sites are shown as black triangles and white arrowheads, respectively. The neomycin (Neo) and the diphtheria toxin (DTA) cassettes for positive and negative selection in ES cells, respectively, are shown. Neo was removed after crossing chimeric mice with animals carrying the Flp-e deleter allele. Deletion using the *CaMKIIalpha-Cre* strain was used to generate the *Tshz3*$^{\Delta}$ allele. UTR: 3' prime untranslated region. (**B**) Lanes 1-3: PCR analysis of mice (lane 1, homozygous wild-type; lane 2, heterozygous *Tshz3*$^{flox/+}$; lane 3, homozygous *Tshz3*$^{flox/flox}$ mutants, using P1 and P2 primers indicated in (**A**)). Lanes 4 and 5, PCR analysis of recombined *Tshz3*$^{\Delta}$ DNA (lane 4, positive product for *Tshz3*$^{\Delta}$ allele using P3 and P2 primers indicated in (**A**); lane 5, markers).

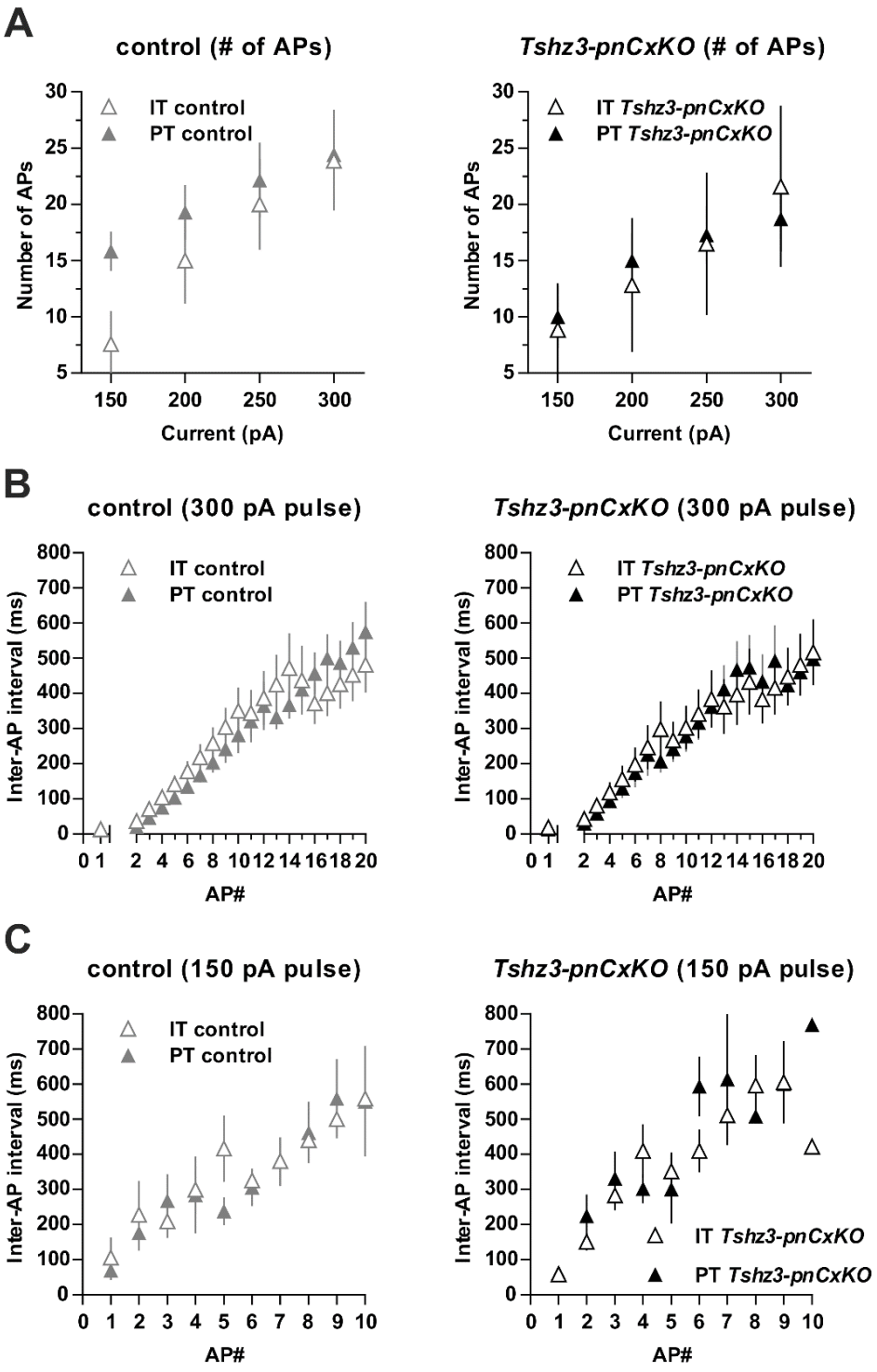

Supplemental Figure S6. AP discharge patterns of IT *vs*. PT CPNs. (**A**) The number of APs emitted by IT *vs*. PT CPNs of the primary motor cortex in response to depolarizing current pulses (800 ms) was similar, both in control (left) and *Tshz3-pnCxKO* (right) mice (IT *vs*. PT control, $F(1,48) = 2.450$, $P = 0.124$; IT *vs*. PT *Tshz3-pnCxKO*, $F(1,44) = 0.01$, $P = 0.921$; two-

way ANOVA). (**B**) During a +300 pA current pulse, the inter-AP interval of IT *vs*. PT CPNs from control (left) and *Tshz3-pnCxKO* (right) mice was similar (IT *vs*. PT control, $F(1,208) = 0.568$, $P = 0.452$; IT *vs*. PT *Tshz3-pnCxKO*, $F(1,188) = 0.067$, $P = 0.792$; two-way ANOVA). (**C**) During a +150 pA current pulse, the inter-AP interval of IT *vs*. PT CPNs from control (left) and *Tshz3-pnCxKO* (right) mice was similar (IT *vs*. PT control, $F(1,65) = 0.227$, $P = 0.635$; IT *vs*. PT *Tshz3-pnCxKO*, $F(1,65) = 1.697$, $P = 0.197$; two-way ANOVA). Data are expressed as means ± s.e.m.

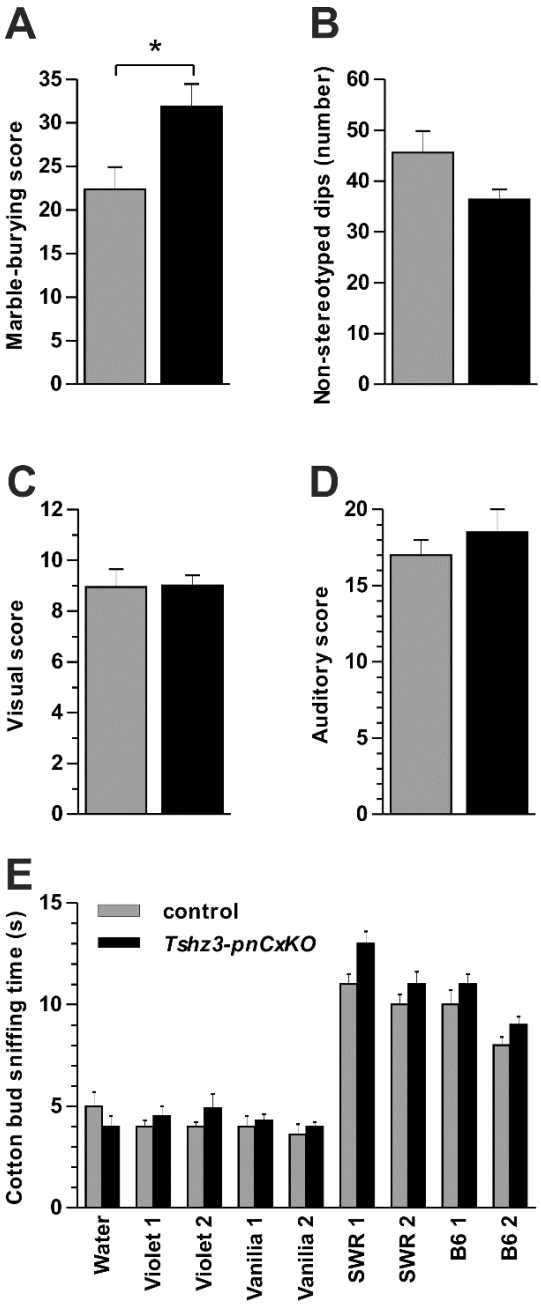

Supplemental Figure S7. Stereotyped behavior and sensory (visual, auditory and olfactory) screening in *Tshz3-pnCxKO* and control mice. *Tshz3-pnCxKO* displayed more stereotyped behaviors than control: (**A**) they buried more marbles ($t(20) = 2.64$, $P = 0.016$, $\eta^2 = 0.24$) when controlled for non-stereotyped dips (**B**). No significant differences were found between the two genotypes for (**C**) visual performance ($t(18) < 1$, $P = 0.60$), (**D**) auditory performance ($t(18) < 1$; $P = 0.65$) and (**E**) olfactory exploration in the habituation/dishabituation test. Time sniffing non-social (water, violet, vanilla) and social (SWR and B6 mice) odors was

analyzed with mixed ANOVA (genotype factor with two levels, *Tshz3-pnCxKO* and control, and 15 odors as repeated measures). The genotype factor was not significant ($F(1, 18) < 1$). n = 11 per group (**A**), n = 10 per group (**B-E**); *$P < 0.01$; data are expressed as means ± s.e.m.

SUPPLEMENTAL TABLES

	control		*Tshz3-pnCxKO*	
	PT	**IT**	**PT**	**IT**
RMP (mV)	-56.45 ± 1.62	-59.16 ± 1.89	-57.30 ± 1.85	-62.94 ± 1.36
AP threshold (mV)	-38.5 ± 1.03	-36.82 ± 1.32	-35.67 ± 0.54	-36.74 ± 1.02
AP amplitude (mV)	106.9 ± 4.19	112.2 ± 4.33	107.2 ± 3.86	117.3 ± 2.33
AP overshoot (mV)	68.4 ± 4.43	75.37 ± 5.13	71.56 ± 4.3	69.01 ± 11.65
AP half-width (ms)	0.84 ± 0.06	0.94 ± 0.03	1.01 ± 0.05	0.93 ± 0.05
AP slope (mV/ms)	170.96 ± 11.54	164.91 ± 8.23	142.43 ± 10.83	160.76 ± 10.69
AP time-to-peak (ms)	0.61 ± 0.03	0.63 ± 0.03	0.66 ± 0.03	0.58 ± 0.02
Input resistance (MΩ)	99.47 ± 6.44	98.11 ± 12.74	120.7 ± 9.55	93.23 ± 8.26
Rheobase (pA)	75.7 ± 7.2	138.6 ± 9.9	101.4 ± 15.7	155.7 ± 29.7

Supplemental Table S1. Electrophysiological properties of L5 CPNs. The electrophysiological properties listed above are similar between PT (pyramidal tract) and IT (intratelencephalic) neurons of the same genotype, as well as between PT or IT of control *vs*. *Tshz3-pnCxKO* (n = 7 PT and 7 IT per genotype. For the RMP (resting membrane potential) and AP (action potential, triggered by +250 pA pulses) properties, $P > 0.05$ for each parameter (1-way ANOVA). For the input resistance (calculated measuring the slope of the linear regression resulting from the current-voltage relationship), $F(3,24) = 1.638$, $P = 0.207$ (1-way ANOVA). For the rheobase, although an overall significant difference [$F(3,24) = 4.09$, $P = 0.018$ (1-way ANOVA)], the Sidak post-test (corrected for FDR - false discovery rate - due to the high data variability) revealed no significant differences in multiple comparisons, i.e. no difference between IT *vs*. PT or between genotypes.

See Excel file "Supplemental Table S2.xlsx"

Supplemental Table S2. Differentially expressed genes (DEGs) in the cerebral cortex of *Tshz3-pnCxKO* mice. (**A**) 1025 DEGs in *Tshz3-pnCxKO* identified with Dseq, edgeR or Desq2. 767 are up-regulated and 258 down-regulated ($P < 0.05$). (**B**) 993 non-ambiguous orthologous human genes. (**C**) 173 (16.7% of 1025) genes encoding postsynaptic density (PSD) proteins from the adult mouse cerebral cortex (MmPSD). (**D**) 176 genes (17.7% of 993) genes encoding PSD proteins from the human cerebral cortex (HsPSD). 167 common proteins between 176 human and 173 mouse PSD lists. 112 (67% of 167) proteins belonging to the consensus HsPSD. 69 ASD-associated proteins (61.6% of 112) belonging to the consensus HsPSD. (**E**) Comparison of the 167 common PSD proteins to the adult mouse DLG4, DLGAP1 and SHANK3 postsynaptic protein-interaction networks identified 17 proteins in the DLG4-, 21 in the DLGAP1- and 16 in the SHANK3-interactome; 9 proteins (BAIAP2, DLGAP3, DLGAP4, GNB1, GRIN2A, GRIN2B, NEFL, SHANK1 and SHANK2) were common to the three protein-interaction networks. (**F**) 741 (74.6% of 993) orthologous human genes involved in brain and nervous system disorders. (**G**) 489 (66% of 741) genes already known or proposed to be involved in ASD. (**H**) 357 (36% of 993) non-ambiguous orthologous human genes with an absolute value of Log2 fold change ($|FC|) > 0.5$ and an adjusted *P*-value (or false discovery rate, FDR) < 0.05. (**I**) 233 (65.3% of 357) genes involved in brain and nervous system disorders. (**J**) 155 (43.4% of 357) ASD-associated genes. (**K**) Ranking of the pathologies; the great majority of these genes (155/357) has been associated with ASD, the second most represented disease being schizophrenia. (**L**) Presynaptic genes.

See Excel file "Supplemental Table S3.xlsx"

Supplemental Table S3. Gene set enrichment analysis. (**A**) Gene Ontology (GO) Biological Process (BP) positive enrichment. (**B**) GO BP negative enrichment. (**C**) GO Cellular Component (CC) positive enrichment. (**D**) GO CC negative enrichment. (**E**) GO Molecular Function (MF) positive enrichment. (**F**) GO MF negative enrichment. (**G**) Panther positive enrichment. (**H**) Panther negative enrichment. (**I**) Reactome positive enrichment. (**J**) Reactome negative enrichment. (**K**) All pathways positive enrichment. (**L**) All pathways negative enrichment. (**M**) Synaptome database (SynaptomeDB) WebGestalt. (**N**) Postsynaptic Pathways (PWs) WebGestalt. (**O**) SynaptomeDB Gene Set Enrichment Analysis (GSEA). (**P**) Postsynaptic Pathways (PWs) GSEA**.** (**Q**) Neurological pathologies GSEA. (**R**) Neurological pathologies (input list for GSEA restricted to |FC| 0.5). (**S**) Neuronal cell types GSEA. (**T**) Complete DESeq2 results**.** (**U**) Ranked genes "mouse" used for GSEA. (**V**) Ranked genes "humanized" used for GSEA**.** (**W**) SynaptomeDB gmt-file used for GSEA. (**X**) Postsynaptic pathways gmt-file used for GSEA. Abbreviations: ES, enrichment score; FDR, false discovery rate; NES, normalized enrichment score.

See Excel file "Supplemental Table S4.xlsx"

Supplemental Table S4. Genes differentially expressed both in P28 *Tshz3-pnCxKO* and E18.5 *Tshz3*$^{lacZ/lacZ}$ mutant cortices. Differentially expressed genes (DEGs) in *Tshz3*$^{lacZ/lacZ}$ ("Tshz3 KO (E18.5)"; blue) and *Tshz3-pnCxKO* ("Tshz3-pnCxKO (P28)"; orange) mutant cortices. Up-regulated genes are shown in red and down-regulated genes in green.

SUPPLEMENTAL REFERENCES

1. Lee EC, Yu D, Martinez de Velasco J, Tessarollo L, Swing DA, Court DL*, et al.* (2001): A highly efficient Escherichia coli-based chromosome engineering system adapted for recombinogenic targeting and subcloning of BAC DNA. Genomics, 73: 56-65.
2. Yagi T, Nada S, Watanabe N, Tamemoto H, Kohmura N, Ikawa Y, Aizawa S (1993): A Novel Negative Selection for Homologous Recombinants Using Diphtheria Toxin-a Fragment Gene. Analytical Biochemistry, 214: 77-86.
3. Liu P, Jenkins NA, Copeland NG (2003): A highly efficient recombineering-based method for generating conditional knockout mutations. Genome Res, 13: 476-484.
4. Casanova E, Fehsenfeld S, Mantamadiotis T, Lemberger T, Greiner E, Stewart AF, Schutz G (2001): A CamKIIalpha iCre BAC allows brain-specific gene inactivation. Genesis, 31: 37-42.
5. Caubit X, Gubellini P, Andrieux J, Roubertoux PL, Metwaly M, Jacq B*, et al.* (2016): TSHZ3 deletion causes an autism syndrome and defects in cortical projection neurons. Nat Genet, 48: 1359-1369.
6. Caubit X, Tiveron MC, Cremer H, Fasano L (2005): Expression patterns of the three Teashirt-related genes define specific boundaries in the developing and postnatal mouse forebrain. J Comp Neurol, 486: 76-88.
7. Kim D, Pertea G, Trapnell C, Pimentel H, Kelley R, Salzberg SL (2013): TopHat2: accurate alignment of transcriptomes in the presence of insertions, deletions and gene fusions. Genome Biol, 14: R36.
8. Langmead B, Salzberg SL (2012): Fast gapped-read alignment with Bowtie 2. Nat Methods, 9: 357-359.
9. Caubit X, Lye CM, Martin E, Core N, Long DA, Vola C*, et al.* (2008): Teashirt 3 is necessary for ureteral smooth muscle differentiation downstream of SHH and BMP4. Development, 135: 3301-3310.
10. Paxinos G, Franklin KBJ (2001): *The Mouse Brain in Stereotaxic Coordinates, 2nd Edition*: Academic Press.
11. Beurrier C, Faideau M, Bennouar KE, Escartin C, Kerkerian-Le Goff L, Bonvento G, Gubellini P (2010): Ciliary neurotrophic factor protects striatal neurons against excitotoxicity by enhancing glial glutamate uptake. PLoS One, 5: e8550.
12. Chassain C, Melon C, Salin P, Vitale F, Couraud S, Durif F*, et al.* (2016): Metabolic, synaptic and behavioral impact of 5-week chronic deep brain stimulation in hemiparkinsonian rats. J Neurochem, 136: 1004-1016.
13. Sprott RL, Staats J (1975): Behavioral studies using genetically defined mice. A bibliography. Behav Genet, 5: 27-82.
14. Sprott RL (1975): Behavioral characteristics of C57BL/6J. DBA/2J, and B6D2F1 mice which are potentially useful for gerontological research. Exp Aging Res, 1: 313-323.
15. Ginsburg B, Allee WC (1942): Some effects of conditioning on social dominance and subordination in inbred strains of mice. PhysiolZool, 15: 485-506.
16. Maxson SC, Canastar A (2003): Conceptual and methodological issues in the genetics of mouse agonistic behavior. Horm Behav, 44: 258-262.
17. Volden PA, Wonder EL, Skor MN, Carmean CM, Patel FN, Ye HG*, et al.* (2013): Chronic Social Isolation Is Associated with Metabolic Gene Expression Changes Specific to Mammary Adipose Tissue. Cancer Prevention Research, 6: 634-645.
18. Thomas A, Burant A, Bui N, Graham D, Yuva-Paylor LA, Paylor R (2009): Marble burying reflects a repetitive and perseverative behavior more than novelty-induced anxiety. Psychopharmacology, 204: 361-373.

19. Makanjuola RO, Hill G, Maben I, Dow RC, Ashcroft GW (1977): An automated method for studying exploratory and stereotyped behaviour in rats. Psychopharmacology (Berl), 52: 271-277.
20. Moy SS, Nadler JJ, Perez A, Barbaro RP, Johns JM, Magnuson TR*, et al.* (2004): Sociability and preference for social novelty in five inbred strains: an approach to assess autistic-like behavior in mice. Genes Brain Behav, 3: 287-302.
21. Nadler JJ, Moy SS, Dold G, Trang D, Simmons N, Perez A*, et al.* (2004): Automated apparatus for quantitation of social approach behaviors in mice. Genes Brain Behav, 3: 303-314.
22. Roubertoux PL, Carlier M, Tordjman S (2015): Deficit in Social Relationships and Reduced Field of Interest in Mice. In: Roubertoux PL, editor. *Deficit in Social Relationships and Reduced Field of Interest in Mice*, New York: Springer, 335-370.
23. Upchurch M, Wehner JM (1988): Differences between Inbred Strains of Mice in Morris Water Maze Performance. Behavior Genetics, 18: 55-68.
24. Vorhees CV, Williams MT (2006): Morris water maze: procedures for assessing spatial and related forms of learning and memory. Nat Protoc, 1: 848-858.
25. Terry AV, Jr., Warner SE, Vandenhuerk L, Pillai A, Mahadik SP, Zhang G, Bartlett MG (2008): Negative effects of chronic oral chlorpromazine and olanzapine treatment on the performance of tasks designed to assess spatial learning and working memory in rats. Neuroscience, 156: 1005-1016.
26. Roubertoux PL, Baril N, Cau P, Scajola C, Ghata A, Bartoli C*, et al.* (2017): Differential Brain, Cognitive and Motor Profiles Associated with Partial Trisomy. Modeling Down Syndrome in Mice. Behav Genet, 47: 305-322.
27. Alamed J, Wilcock DM, Diamond DM, Gordon MN, Morgan D (2006): Two-day radial-arm water maze learning and memory task; robust resolution of amyloid-related memory deficits in transgenic mice. Nat Protoc, 1: 1671-1679.
28. Lipp HP, Wahlsten D (1992): Absence of corpus callosum. In: Driscoll P, editor. *Absence of corpus callosum*, Boston, USA: Birkhauser,
29. Yang M, Crawley JN (2009): Simple behavioral assessment of mouse olfaction. Curr Protoc Neurosci, Chapter 8: Unit 8 24.